Near field sampling of conformal sources

Raffaele Moretta*[(1)], Giovanni Leone[(1)]
(1) Dipartimento di Ingegneria, Università degli Studi della Campania "L. Vanvitelli", Aversa, 81031, Italia

Abstract

In this paper, the question of sampling the near field of conformal sources is addressed for some source and observation geometries. At first, the minimum number of sampling points required to discretize the near field without loss of information is computed by an analytical evaluation of the number of degrees of freedom (NDF). Then, the location of the field samples is found and an interpolation formula is provided.
The analysis is performed for a 2D scalar geometry consisting of an elliptical/parabolic arc source whose radiated field is observed over a circumference arc in near zone.

1. Introduction

The issue of sampling the field radiated by a source or scattered by an object is a classical problem of the electromagnetics literature [1, 2, 3]. In particular, the development of a proper sampling scheme is useful not only to represent the radiated/scattered field but also in other applications like antenna testing, source reconstruction, and imaging problems [4, 5].
Over the years several sampling schemes have been proposed for the planar, cylindrical, and spherical scanning systems. Most of them define the field discretization step by relying on general knowledge about the source, as the overall electrical dimensions. Despite this, the questions of finding

- the minimum number of samples to discretize the radiated field without loss of information,
- the locations of the sampling points

are still open for many source and observation geometries. Since the NDF provides the minimum number of parameters required to represent the field with good accuracy, the achievement of the above points can be recast as finding a sampling grid employing a number of field samples essentially equal to the NDF.
As concerns the radiated field, sampling schemes adopting a non-redundant number of field samples have been proposed in [6, 7, 8] for the case of planar sources whose radiated field is observed over a plane.
Here, the attention is focused on the sampling of the field radiated by conformal antennas and, for sake of simplicity, a 2D geometry consisting of an elliptical or a parabolic arc source is considered.

For a source with a general shape, a common sampling criterion consists in collecting the radiated field with a uniform step in $M_{upper} = 2\,\beta a\,\theta_{max}/\pi + 1$ points [9] where β is the wavenumber, a the radius of the smallest circle enclosing the source, and $2\theta_{max}$ is the extension of the angular sector on which the radiated field is collected. However, such sampling scheme requires collecting a redundant number of points since it does not take into account the source shape. Here, by exploiting the same approach adopted in [10] for the case of a circumference arc source, a non-uniform sampling scheme employing a number of field samples essentially equal to the NDF is devised for the elliptical and the parabolic arc sources. This study generalizes the far-field results provided in [11] to the case of near field observation domain.

2. Geometry of the problem

In this paper, the 2D scalar geometry depicted in Fig. 1 is considered.

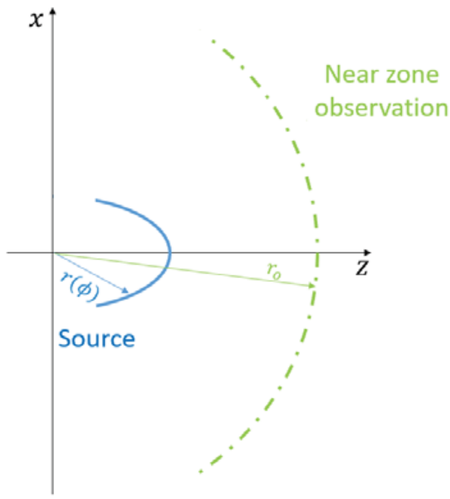

Figure 1. Geometry of the problem

An electric current $\boldsymbol{J}$, directed along the $y-$axis, is supported over a curve $\boldsymbol{\gamma}$ lying in the plane zx representing an elliptic or a parabolic arc. Accordingly, if a focus of the arc source is placed at the origin of the reference system, the $\boldsymbol{\gamma}$ curve can be represented in the polar coordinates $r(\phi)$ and ϕ as

$$\boldsymbol{\gamma}(\phi) = (\,r(\phi)\,cos\phi, r(\phi)\,sin\phi\,) \tag{1}$$

where

$$r(\phi) = \frac{p}{1 + e\, cos\phi} \qquad (2)$$

with $\phi \in [-\phi_{max}, \phi_{max}]$.
In particular, for a parabolic arc, p is twice the focal length and $e = 1$. Instead, for an elliptic arc, p is the semi-latus rectum and $0 < e < 1$ is the eccentricity.
The corresponding electric field radiated has only the $y-$ component which is observed over an arc of circumference of radius r_o located in near non-reactive zone. For the geometry at the hand, the component of the radiated field can be expressed as

$$E(\theta) = TJ(\phi) \qquad (3)$$

where the radiation operator

$$T : L_2([-\phi_{max}, \phi_{max}]) \rightarrow E \in L_2([-\theta_{max}, \theta_{max}])$$

is given by

$$TJ(\phi) = \int_{-\phi_{max}}^{+\phi_{max}} J(\phi) \frac{e^{-j\,\beta\, R(\phi,\theta)}}{\sqrt{R(\phi,\theta)}} \|\boldsymbol{\gamma}'(\phi)\|\, d\phi \qquad (4)$$

with

$$R(\phi,\theta) = \sqrt{r_o^2 + r_s^2(\phi) - 2 r_o r_s(\phi) \cos(\theta - \phi)} \qquad (5)$$

and $\|\boldsymbol{\gamma}'(\phi)\|$ denoting the norm of the derivative of $\boldsymbol{\gamma}'(\phi)$.
Then, a weight adjoint operator can be defined as

$$T_w^\dagger E = \|\boldsymbol{\gamma}'(\phi)\| \int_{-\phi_{max}}^{+\phi_{max}} w(\phi,\theta) \frac{e^{j\,\beta\, R(\phi,\theta)}}{\sqrt{\beta R(\phi,\theta)}} E(\theta) d\theta \qquad (6)$$

where $w(\phi,\theta)$ denotes a weight function.
The latter represents the only difference between $T_w^\dagger$ and the usual adjoint $T^\dagger$.

3. Overview of the paper

The goals of the paper are: 1) to evaluate the NDF of the radiated field, 2) to find the positions of the field samples that allow interpolating the near field with only NDF samples. Such goals can be reached by introducing the operator $TT_w^\dagger$ and studying the eigenvalue problem $TT_w^\dagger v_n = \sigma_n^2 v_n$ which can be explicitly written as

$$\int_{-\theta_{max}}^{\theta_{max}} K(\theta_o,\theta) v_n(\theta)\, d\theta = \sigma_n^2\, v_n(\theta_o) \qquad (7)$$

where $K(\theta_o,\theta)$, $\{\sigma_n^2\}$ and $\{v_n\}$ denote respectively the kernel, the eigenvalues and the eigenfunctions of $TT_w^\dagger$.
In particular, the kernel function is given by

$$K(\theta_o,\theta) = \int_{-\phi_{max}}^{\phi_{max}} w(\phi,\theta) \|\boldsymbol{\gamma}'(\phi)\|^2 \frac{e^{-j\beta[R(\phi,\theta_o) - R(\phi,\theta)]}}{\sqrt{R(\phi,\theta_o)\, R(\phi,\theta)}} d\phi \qquad (8)$$

As concerns the NDF of the near field, it can be found by computing the number of relevant eigenvalues of $TT_w^\dagger$.
Instead, the second goal can be achieved by recasting $TT_w^\dagger$ as a convolution operator with a bandlimited kernel through a change of variables. Then, the spacing between the sampling points is found by deriving the sampling step from the bandwidth of the kernel; instead, an interpolation formula of the radiated field is derived by the application of the Shannon sampling theorem.

All the steps required to achieve the above-mentioned goals are summarized in the block diagram in Fig. 2.

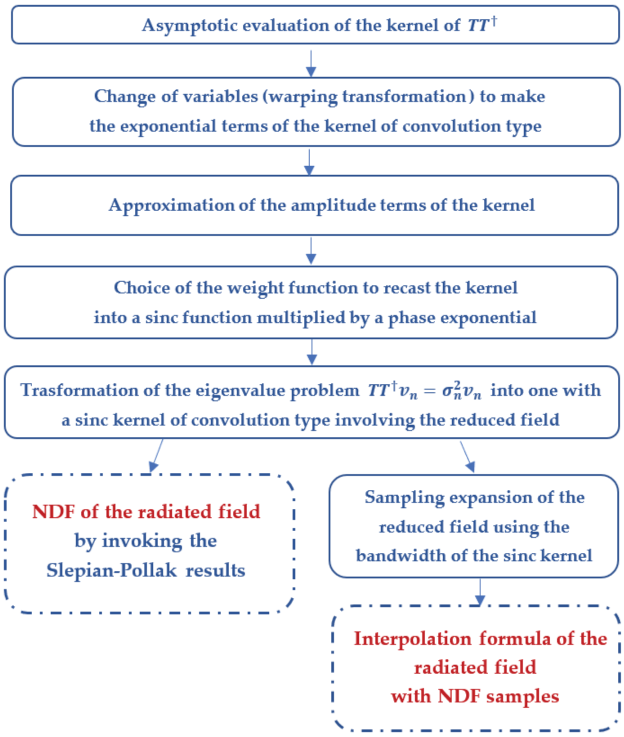

Figure 2. Steps required to compute the NDF and to provide an interpolation series of the near field.

4. Study of the operator $TT^\dagger$

In order to evaluate the kernel of $TT_w^\dagger$, let us rewrite it as

$$K(\theta_o,\theta) = \int_{-\phi_{max}}^{\phi_{max}} w(\phi,\theta) A(\phi,\theta_o,\theta)\, e^{-j\beta p\, \Psi(\phi,\theta_o,\theta)}\, d\phi \qquad (9)$$

where

$$A(\phi,\theta_o,\theta) = \frac{\|\gamma'(\phi)\|^2}{\sqrt{R(\phi,\theta)R(\phi,\theta_o)}}, \quad \Psi(\phi,\theta_o,\theta) = \frac{R(\phi,\theta_o) - R(\phi,\theta)}{p}.$$

For each $\theta \neq \theta_o$, if $\beta p \gg 1$ the kernel function can be evaluated with an asymptotic technique. In particular, in absence of stationary points, the kernel function $K(\theta_o,\theta)$ can be approximated by the contributions of the endpoints. This returns

$$K(\theta_o,\theta) \approx \frac{w(\phi_{max},\theta)\, A(\phi_{max},\theta_o,\theta)}{-j\beta p\, \Psi'(\phi_{max},\theta_o,\theta)} e^{-j\beta p\, \Psi'(\phi_{max},\theta_o,\theta)} - \frac{w(-\phi_{max},\theta_o) A(-\phi_{max},\theta_o,\theta)}{-j\beta p\, \Psi'(-\phi_{max},\theta_o,\theta)} e^{-j\beta p\, \Psi'(-\phi_{max},\theta_o,\theta)} \qquad (10)$$

with Ψ' denoting the derivative of Ψ with respect to ϕ.
In the couple of variables (θ_o,θ), the kernel function is not convolution (i.e., it does not depend on the difference $\theta_o - \theta$). To make $TT_w^\dagger$ more similar to a convolution operator, let us introduce the following functions

$$\eta(\theta_o) = \frac{R(-\phi_{max},\theta_o) - R(\phi_{max},\theta_o)}{2p} \qquad (11)$$

$$\gamma(\theta_o) = \frac{R(-\phi_{max},\theta_o) + R(\phi_{max},\theta_o)}{2p} \qquad (12)$$

In the variables $\eta_o = \eta(\theta_o)$ and $\eta = \eta(\theta)$, the kernel function can be rewritten as

$$K(\eta, \eta_o) = -\, e^{-j\,\beta p\,(\gamma(\eta_o) - \gamma(\eta))} \frac{d\theta}{d\eta} \left(\frac{w(\phi_{max}, \eta)\, A(\phi_{max}, \eta_o, \eta)}{j\beta p\, \Psi'(\phi_{max}, \eta_o, \eta)} e^{j\,\beta p\,(\eta_o - \eta)} - \frac{w(-\phi_{max}, \eta)\, A(\phi_{max}, \eta_o, \eta)}{j\beta p\, \Psi'(-\phi_{max}, \eta_o, \eta)} e^{-j\,\beta p\,(\eta_o - \eta)} \right) \quad (13)$$

where the factor $d\theta/d\eta$ is the Jacobian arising from the change of variable.

At this juncture, the phase exponential are convolution but the kernel has still an intricate structure. However, if the numerator and the denominator of the amplitude term A/Ψ' are expanded with respect to η_o in a Taylor series stopped at the first non-zero term, it results that

$$\frac{A(\phi_{max}, \eta_o, \eta)}{\Psi'(\phi_{max}, \eta_o, \eta)} \approx \frac{A(\phi_{max}, \eta, \eta)}{\frac{d\Psi'(\phi_{max}, \eta_o, \eta)}{d\theta_o} \frac{d\theta}{d\eta_o}\Big|_{\eta_o = \eta} (\eta_o - \eta)} \quad (14)$$

$$\frac{A(-\phi_{max}, \eta_o, \eta)}{\Psi'(-\phi_{max}, \eta_o, \eta)} \approx \frac{A(-\phi_{max}, \eta_o, \eta_o)}{\frac{d\Psi'(-\phi_{max}, \eta_o, \eta)}{d\theta_o} \frac{d\theta}{d\eta_o}\Big|_{\eta_o = \eta} (\eta_o - \eta)} \quad (15)$$

Hence, if the weight function is chosen ab initio as

$$w(\phi, \theta) = \frac{1}{A(\phi, \theta, \theta)} \frac{d\Psi'(\phi, \theta_o, \theta)}{d\theta_o}\Big|_{\theta_o = \theta} \quad (16)$$

then the kernel function can be rewritten in form below

$$K(\eta_o, \eta) = -2 e^{-j\beta p\,(\gamma(\eta_o) - \gamma(\eta))}\, sinc\big(\beta p (\eta_o - \eta)\big) \quad (17)$$

Accordingly, the eigenvalue problem $\boldsymbol{T T_w^\dagger v_n = \sigma_n^2 v_n}$ can be now expressed as

$$\int_{\eta(-\theta_{max})}^{\eta(\theta_{max})} -2\, e^{-j\beta p\,(\gamma(\eta_o) - \gamma(\eta))}\, sinc\big(\beta p\, (\eta_o - \eta)\big) v_n(\eta)\, d\eta = \sigma_n^2 v_n(\eta_o). \quad (18)$$

5. NDF of the near field

In this section the NDF of the near field are computed by evaluating the number of relevant eigenvalues of (18). To achieve this goal, let us fix

$$\tilde{v}_n(\eta_o) = e^{\,j\,\beta p\,\gamma(\eta_o)}\, v_n(\eta_o) \quad (19)$$

Thanks to (19), Equation (18) can be rewritten as

$$\int_{\eta(-\theta_{max})}^{\eta(\theta_{max})} -2\, sinc\big(\beta p(\eta - \eta_o)\big)\, v_n(\eta)\, d\eta = \sigma_n^2 v_n(\eta_o) \quad (20)$$

The eigenvalues behavior of (20) was largely investigated by Slepian-Pollak in [12]. In particular, they showed that the eigenvalues of (20) exhibit a step-like behavior with the knee occurring at the index

$$N = \frac{2\beta p}{\pi} \eta(\theta_{max}) = \frac{\beta [R(-\phi_{max}, \theta_{max}) - R(\phi_{max}, \theta_{max})]}{\pi} \quad (21)$$

Such a number represents an analytical evaluation of the NDF of the near field.

6. Sampling of the near field

At this juncture, the aim is to provide an interpolation formula of the near field that exploits a number of field samples essentially equal to the NDF.

By virtue of (20), the eigenfunctions $\{\tilde{v}_n(\eta_o)\}$ are bandlimited functions with respect to η_o with a bandwidth βp. Accordingly, for each n, they can be represented through the following truncated sampling series

$$\tilde{v}_n(\eta_o) \approx \sum_{m=-M_o}^{M_o} \tilde{v}_n(\eta_{om})\, sinc(\beta a\, \eta_o - m\pi) \quad (22)$$

where $\eta_m = m\frac{\pi}{\beta p}$ and $M_o = \frac{\beta p}{\pi} \eta(\theta_{max})$.

It is worth remarking that the maximum and the minimum value of the index m is chosen in such a way that only the samples falling into the set $[\eta(-\theta_{max}), \eta(\theta_{max})]$ are taken into account. By considering (19) and (22), it results that the eigenfunctions $\{v_n(\eta_o)\}$ can be expressed as below

$$v_n(\eta_o) \approx e^{-\,j\,\beta p\,\gamma(\eta_o)} \sum_{m=-M_o}^{M_o} v_n(\eta_{om})\, e^{\,j\,\beta p\,\gamma(m\Delta\eta)}\, sinc(\,\beta p\, \eta_o - m\pi\,) \quad (23)$$

Since the near field can be written as a linear combination of the eigenfunctions $v_n\,(\eta_o)$, it results that the near field can be approximating through the following approximation

$$E(\eta_o) \approx e^{-\,j\,\beta p\,\gamma(\eta_o)} \sum_{m=-M_o}^{M_o} E(\eta_{om})\, e^{\,j\,\beta p\,\gamma(m\Delta\eta)}\, sinc(\,\beta p\, \eta_o - m\pi\,) \quad (24)$$

The field samples appearing in (24) are uniformly arranged in the variable η_o. However, since the function $\eta(\theta_o)$ is nonlinear, they result non-uniform arranged in the variable θ_o. In order to find the exact location of the field samples in the variables θ_o, the equation

$$\eta(\theta_{om}) = m\frac{\pi}{\beta p} \quad (25)$$

must be solved for each $m \in \{-M_o, \dots, M_o\}$.

7. Numerical results

In this section, a numerical validation of (21) and (24) is performed by a numerical analysis.

An elliptic arc source with $p = 60\lambda$ and $e = 0.9$ spanning the interval $[-\phi_{max}, \phi_{max}] = [-40°, 40°]$ is considered. The source current is chosen in such a way to focus at $\theta = \theta^* = 10°$, accordingly

$$J(\phi) = e^{-j\,\beta\, r(\phi) \cos(\theta^* - \phi)} \quad (26)$$

The near field is observed over a circumference arc of radius $r_o = 45\lambda$ subtending the angular sector $[-\theta_{max}, \theta_{max}] = [-47°, 47°]$.

In Fig. 3, the eigenvalues of $TT^\dagger$ are compared with those of $TT_w^\dagger$. It can be noted that the use of a weighted adjoint changes the behavior of the eigenvalues but not the index at which they decay abruptly. The latter is predicted by (21) which, in the considered test case, returns $N = 90$ in perfect agreement with Fig. 3.

In Fig. 4, the optimal sampling points of the near field are shown. As predict by (25), the sampling points are non-uniformly spaced along the observation domain; in particular, they are larger by moving towards the edges of the observation domain.

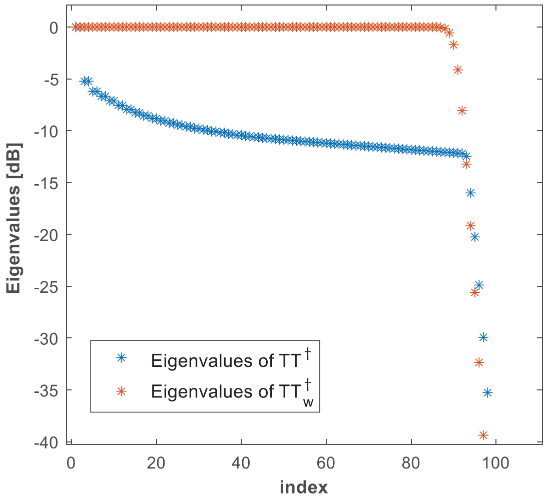

Figure 3. Comparison between the eigenvalues of $TT^\dagger$ and those of $TT_w^\dagger$.

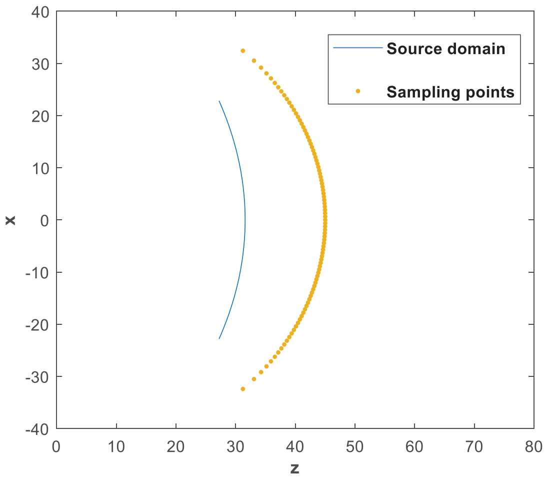

Figure 4. Sampling points of the proposed strategy.

In Fig. 5, the exact near field computed by the radiation operator (3) is compared with the field returned by the interpolation formula (24).

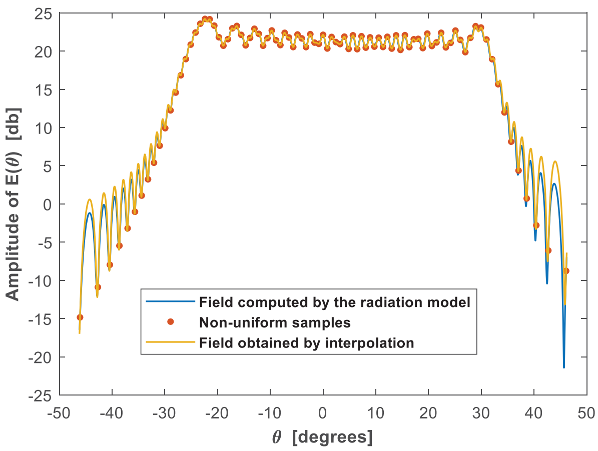

Figure 5. Source domain and sampling points of the proposed strategy.

As can be seen from Fig. 5, despite the interpolation formula (24) exploits only $N+1=91$ non-uniform field samples, the interpolated field agrees very well with the exact field with a relative error equal to 2.6 %.

8. Conclusion

In this paper, the question of efficiently sampling the near field radiated by parabolic or elliptical source arcs has been addressed. In particular, at first, the minimum number of field measurements required to discretize the near field without loss of information has been computed. Then, the location of the sampling points has been found and an interpolation formula of the near field employing a number of samples essentially equal to the NDF has been provided. Accordingly, the proposed sampling scheme allows reducing at minimum the number of field samples and this positively affects the acquisition time in near field measurement techniques.

References

[1] E. Joy, D. Paris, “Spatial sampling and filtering in near-field measurements,” *IEEE Trans. Antennas Propag.*, vol. *20*, no. 3, pp. 253–261, 1972.

[2] O. M. Bucci, C. Gennarelli, C. Savarese, "Representation of electromagnetic fields over arbitrary surfaces by a finite and nonredundant number of samples," *IEEE Trans. Antennas Propag.*, vol. 46, no. 3, pp. 351-359, 1998.

[3] B. Hofmann, O. Neitz, T. Eibert, “On the minimum number of samples for sparse recovery in spherical antenna near-field measurements,” *IEEE Trans. Antennas Propag.*, vol. *67*, no. 12, pp. 7597–7610, 2019

[4] G. Ruvio, R. Solimene, A. D'Alterio, M.J. Ammann, R. Pierri, “RF breast cancer detection employing a non-characterized vivaldi antenna and a MUSIC-inspired algorithm. *International Journal of RF and Microwave Computer-Aided Engineering*, vol. 23, no. 5, pp. 598-609, 2013.

[5] R. Solimene, A. Brancaccio, J. Romano, R. Pierri, "Localizing Thin Metallic Cylinders by a 2.5-D Linear Distributional Approach: Experimental Results," *IEEE Trans. Antennas Propag.*, vol. 56, no. 8, pp. 2630-2637, 2008.

[6] A. Capozzoli, C. Curcio, A. Liseno, P. Vinetti, “Field sampling and field reconstruction: a new perspective”, *Radio Sci.*, vol. 45, RS6004, 2010.

[7] M.A. Maisto, R. Pierri, R. Solimene, “Near-Field Warping Sampling Scheme for Broad-Side Antenna Characterization,” *Electronics*, vol. *9*, no. 6, art. no. 1047, 2020.

[8] R. Pierri, R. Moretta, “Asymptotic study of the radiation operator for the strip current in near Zone,” *Electronics*, vol. 9, no. 6, art. no. 911, 2020.

[9] G. Leone, M.A. Maisto, R. Pierri, "Inverse source of circumference geometries: SVD investigation based on Fourier analysis." *Progress In Electromagnetics Research M,* vol. 76, pp. 217-230, 2018.

[10] R. Moretta, G. Leone, F. Munno, R. Pierri, “Optimal field sampling of arc sources via asymptotic study of the radiation operator,” *Electronics*, vol. 11, no. 2, art. no. 270, 2022.

[11] G. Leone, F. Munno, R. Pierri, "Inverse source on conformal conic geometries," *IEEE Trans. Antennas Propag.*, vol. 69, no. 3, pp. 1596-1609, 2021.

[12] D. Slepian, H.O. Pollack, “Prolate spheroidal wave functions, Fourier analysis, and uncertainty - I,” *Bell Syst. Tech. J.*, vol. *40*, no. 1, pp. 43, 1961.